



日本原子力研究開発機構機関リポジトリ
Japan Atomic Energy Agency Institutional Repository

Title	Analysis of the electric double layer structure formed in an ionic liquid using neutron reflectivity
Author(s)	Tamura Kazuhisa, Akutsu-Suyama Kazuhiro, Cagnes M., Darwish T. A.
Citation	ECS Advances, 1(2), p. 020503_1-020503_5
Text Version	Published Journal Article
URL	https://jopss.jaea.go.jp/search/servlet/search?5073110
DOI	https://doi.org/10.1149/2754-2734/ac6963
Right	© 2022 The Author(s). Published on behalf of The Electrochemical Society by IOP Publishing Limited. This is an open access article distributed under the terms of the Creative Commons Attribution 4.0 License (CC BY, http://creativecommons.org/licenses/by/4.0/), which permits unrestricted reuse of the work in any medium, provided the original work is properly cited.

OPEN ACCESS

Analysis of the Electric Double Layer Structure Formed in an Ionic Liquid Using Neutron Reflectivity

To cite this article: Kazuhisa Tamura *et al* 2022 *ECS Adv.* 1 020503

View the [article online](#) for updates and enhancements.

Measure the electrode expansion in the nanometer range.
Discover the new electrochemical dilatometer ECD-4-nano!

EL-CELL[®]
electrochemical test equipment



- PAT series test cell for dilatometric analysis (expansion of electrodes)
- Capacitive displacement sensor (range 250 μm , resolution ≤ 5 nm)
- Optimized sealing concept for high cycling stability

www.el-cell.com +49 (0) 40 79012 737 sales@el-cell.com





Analysis of the Electric Double Layer Structure Formed in an Ionic Liquid Using Neutron Reflectivity

Kazuhisa Tamura,^{1,*} Kazuhiro Akutsu-Suyama,² Marina Cagnes,³ and Tamim A. Darwish³

¹Materials Sciences Research Center, Japan Atomic Energy Agency, Hyogo 679-5148, Japan

²Research Center for Neutron Science and Technology, Comprehensive Research Organization for Science and Society (CROSS), Ibaraki, 319-1106, Japan

³Australian Centre for Neutron Scattering and National Deuteration Facility, Australian Nuclear Science and Technology Organization (ANSTO), Kirrawee DC, NSW 2232, Australia

The ionic liquid/Si electrode interface was investigated using neutron reflectivity. We precisely elucidated the structure of the electrical double layer formed at 1-butyl-3-methylimidazolium bis(trifluoromethylsulfonyl)amide ([BMIM]TFSA)/Si(100) electrode interface with the orientation of the [BMIM]TFSA molecule using a partially deuterated [BMIM]TFSA. The results revealed that [BMIM]TFSA molecules form a layered structure. Cation and anion molecules are alternately stacked and molecules in the first three layers are horizontally oriented to the electrode surface at $E = -1.2$ V, i.e., on the negatively charged electrode surface. It was also revealed that the imidazole ring in [BMIM] cation is parallel to the electrode surface.

© 2022 The Author(s). Published on behalf of The Electrochemical Society by IOP Publishing Limited. This is an open access article distributed under the terms of the Creative Commons Attribution 4.0 License (CC BY, <http://creativecommons.org/licenses/by/4.0/>), which permits unrestricted reuse of the work in any medium, provided the original work is properly cited. [DOI: 10.1149/2754-2734/ac6963]



Manuscript submitted January 31, 2022; revised manuscript received April 21, 2022. Published May 12, 2022.

Supplementary material for this article is available [online](#)

An ionic liquid (IL) is a salt that is liquid at room temperature. The salts are organic compounds that have low vapor pressure, a wide electrochemical window, high conductivity, and so on.¹ Furthermore, the physical properties of ILs can be easily tuned by the molecular structure. As a result, ILs have gained attention as a “third solvent” in various fields of research. One application of an IL is as an electrolyte in electrochemical devices, such as batteries and capacitors.² Therefore, ILs for Li-ion batteries and fuel cells have been extensively studied.^{3–5} However, it becomes obvious that the electrochemical reactions which occur in ILs differ from those that occur in water electrolytes. Particularly, in electrodeposition reactions, the deposit looks different from that obtained by water electrolytes.^{6,7} Furthermore, underpotential deposition does not occur in ILs, except for in metals such as Bi and Sb.^{8,9} These differences are thought to be owing to the differences in the structure of the electric double layer (EDL) as well as the different solvation state of the metal ions.¹⁰ As is well known, to control electrochemical reaction precisely we have to understand the electrode/electrolyte interface including EDL structure in detail and this fact is also applicable to ILs. Therefore, the analysis of EDL structure has been one of the important topics in studies of electrochemical reactions in ILs.

In ILs, the Debye–Hückel limiting law cannot be applied owing to the high ionic strength. Therefore, EDL may not possess a Gouy–Chapman type structure.¹¹ In the past decade, many studies to determine the structure of the EDL have been performed using quantum beam techniques,^{12–15} scanning probe microscope techniques,¹⁶ spectroscopic techniques,^{17–19} and theoretical calculations.^{20,21} It was reported that IL molecules form a layered structure on the charged surface,¹² depending on the surface charge (i.e., electrode potential). Furthermore, a large hysteresis was observed on the reordering of the molecules in the layers.¹⁸ On the other hand, the structure of EDL formed in ILs was not still fully understood since it should be largely different from that formed in aqueous electrolytes as described above and methods for studies of EDL are limited, indicating that it must be studied using various techniques and results must be discussed from many perspectives.

We have investigated the IL/electrode interface using quantum beam measurements. We previously studied the structure of Au(111) electrode surface in neat 1-butyl-3-methylimidazolium bis(trifluoromethylsulfonyl)amide ([BMIM]TFSA) and 1-butyl-1-methylpyrrolidinium bis(trifluoromethylsulfonyl)amide ([BMP]TFSA) and their ILs containing halide anions using surfacer X-ray scattering (SXS). ILs, which consist of TFSA anion, are highly hydrophobic and it is easy to handle; therefore, they are suitable for industrial applications and studied from many points of view. In our studies, it was found that IL molecules adsorb on Au(111) electrode surface and the structure of Au(111) electrode surface is governed by adsorbed IL molecules.²² Further, it was found that halide anions are coadsorbed with IL molecules and increase the mobility of surface atoms; however, the surface structure is mainly governed by adsorbed IL molecules.²³ These studies proved that quantum beam measurements are suitable for the analysis of the structure of the IL/electrode interface since they are non-destructive techniques and measurements can be carried out under electrochemically ideal conditions. We have subsequently investigated the structure of EDL formed in [BMIM]TFSA on Si(100) electrode surface using neutron reflectivity. In our previous study, we developed a deuteration method for imidazolium IL with a systematically controlled deuteration level. We further studied the structure of EDL formed in fully deuterated [BMIM]TFSA using neutron reflectivity and preliminarily proved that IL molecules form layered structure in EDL.²⁴

Reflectivity using quantum beams (X-ray and neutron) is a technique that can reveal the structure of thin films on the atomic scale.²⁵ Thickness, roughness, and composition can be obtained. Samples can be not only single-layer films but also multi-layer films.

Both X-ray reflectivity (XR) and NR are common techniques. The difference between the two is that an X-ray interacts with an electron in an atom, whereas a neutron interacts with a nucleus. This is reflected in the difference in the atomic scattering factors (ASF) (note that it is called scattering length density (SLD) for neutrons). The ASF value is proportional to the atomic number, therefore, it is small for light elements. On the other hand, the SLD value is element selective, i.e., it does not depend on the atomic number and can result in a large SLD value even for light elements. Therefore, the NR technique is ideally suitable for the structural analysis of soft materials, which consist of light elements. In electrochemistry, the NR technique is used for the analysis of the structure of solid electrolyte interphase (SEI), which consist of Li^+ and decomposition

*Electrochemical Society Member.

²E-mail: tkazu@spring8.or.jp

product of electrolyte, formed on the electrode surface of Li-ion batteries.^{26,27}

Additionally, the SLD value of compounds can be tuned through isotope substitution.²⁸ For example, H and D atoms have a negative and positive value for scattering length, respectively. Organic compounds generally contain H atoms; therefore, it is easy to tune the SLD value of organic compounds by deuteration. The difference of the SLD value between the materials is known as the contrast. Precise structural analysis can be carried out with the optimization of the contrast using deuteration.²⁹ In the same manner, if there is enough contrast inside a molecule, it is possible to explicitly distinguish the orientation of the IL molecule in EDL.

In this paper, we studied the EDL structure formed in an IL using the NR technique to reveal the orientation of IL molecules adsorbed on the negatively charged electrode surface, where many useful depositions occur. In detail, we studied the EDL structure with the orientation of IL molecules adsorbed on a Si(100) electrode surface in a finely deuterated [BMIM]TFSA using the NR technique under electrochemically ideal conditions. NR measurements revealed that the [BMIM]TFSA molecules form a layered structure. Both cation and anion molecules in EDL are horizontally oriented to the electrode surface and the imidazole ring in [BMIM] cation is parallel to the electrode surface.

Experimental

An n-Si(100) disk was used as the working electrode. The size used for NR and electrochemical impedance spectroscopy (EIS) was 40 mm (l) × 40 mm (w) × 3 mm (t) and 10 mm (l) × 15 mm (w) × 0.5 mm (t), respectively. In this study, the native oxide was not removed to avoid the surface composition change by the oxide formation during electrochemical measurements.³⁰ The reference and counter electrodes were Pt wires and the electrolyte was [BMIM]TFSA. For NR measurements, partially deuterated [BMIM]TFSA (*d*-[BMIM]TFSA) was synthesized using Pd/Pt catalysts.²⁴ All hydrogen atoms in the imidazole ring and the methyl group were fully deuterated and 48.9% of hydrogen in the butyl group was deuterated. To reveal the orientation of the cations adsorbed on the Si electrode surface, the SLD value of the butyl group was altered to the SLD value of TFSA. *d*-[BMIM]TFSA was dehydrated at 80 °C under vacuum for 24 h before use.

Before the measurement, the working electrode was sonicated in acetone and ethanol, followed by rinsing with mill-Q water. After the cleaning procedure, it was transferred to a glovebox filled with Ar gas (dew point < -80 °C) and dried in the glove box for over 20 min. The reference and counter electrodes were annealed and transferred to the glovebox. The electrochemical cell was built, and the IL was introduced to the cell in the glovebox. The design of the electrochemical cell for the NR measurement is based on the cell proposed by Yonemura et al.³¹ Figure 1 shows a schematic cross-sectional view of the NR-cell. The reference electrode (RE) and the counter electrode (CE) were approximately 30 mm long and were parallelly arranged at the center of the cell to cover the irradiation area. The distance between the working and the reference (RE)/counter (CE) electrodes was 2–3 mm to minimize solution resistance. The electrode potential was controlled by a potentiostat (IviumStat, Ivium technology).

NR measurements were conducted at BL17 (SHARAKU), the Materials and Life Science Experimental Facility of the J-PARC. The neutron beam was introduced from the side of the n-Si(100) electrode as shown in Fig. 1 to avoid the absorption of a neutron by IL and minimize the background scattering. A 25 mm beam footprint was maintained on the sample surface by using six different kinds of incident slits. The covered Q_z range was 0.005–0.23 Å⁻¹, in which $Q_z = (4\pi/\lambda)\sin\theta$ (here, θ represents the incident angle). All the measurements were performed at room temperature. The data reduction, normalization, and subtraction were performed using a program installed in BL17 SHARAKU. The electrode potential was stepped to the desired potential and was maintained for 10 min to

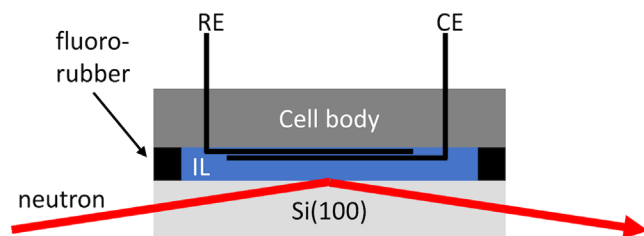


Figure 1. A schematic cross-sectional view of the electrochemical cell for NR measurements.

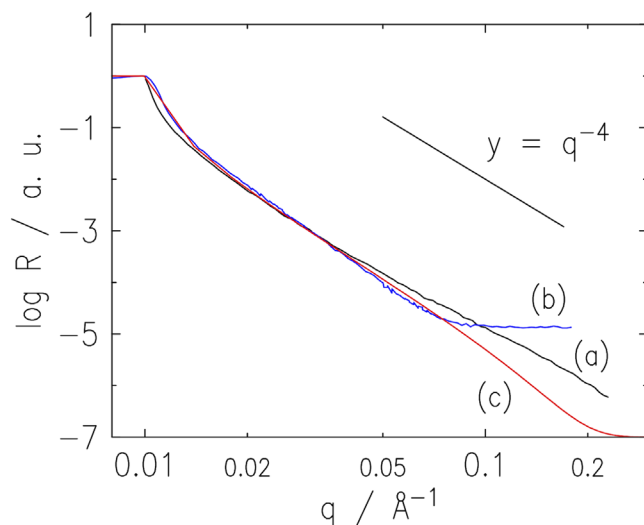


Figure 2. Reflectivity profiles measured in (a) air and (b) the partially deuterated [BMIM]TFSA at $E = -1.2$ V and (c) simulated for a bulk structure model.

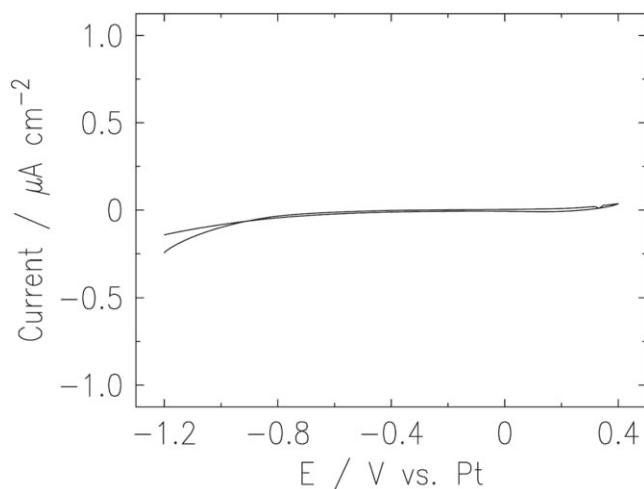


Figure 3. Cyclic voltammogram of the native oxide covered n-Si(100) electrode measured in the partially deuterated [BMIM]TFSA (scan rate = 2 mV s⁻¹).

reach the equilibrium interface structure.¹⁷ Then, the accumulation of reflectivity intensity was started. In the fitting analysis of the NR profile, SLD values of *d*-[BMIM]TFSA were calculated based on the molar volume of molecule³² and SLD values of elements.³³

Results and Discussion

To increase the reliability of the reflectivity profiles, a sample must have a flat and large-area surface. Furthermore, with respect to

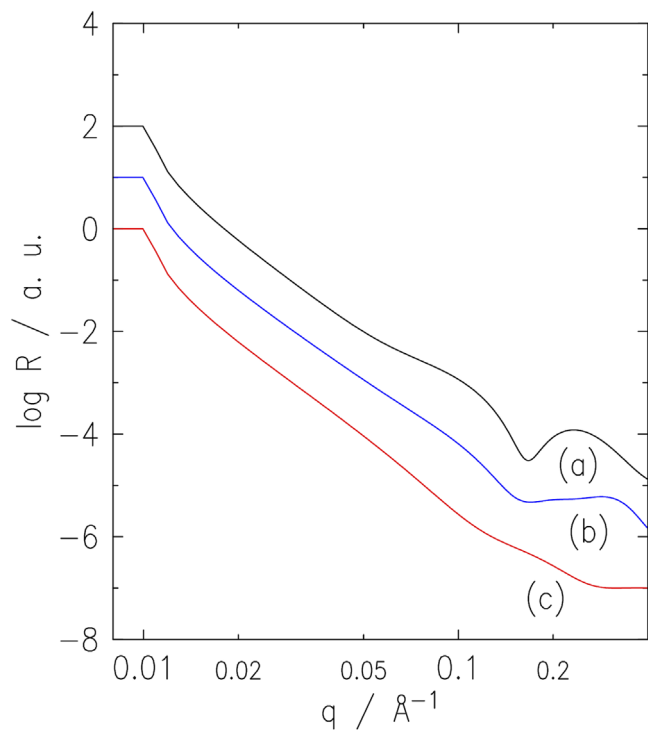


Figure 4. Simulated reflectivity profiles: (a) imidazole ring down, (b) butyl group down, and (c) edge-on structures.

electrochemistry, a non-reactive and stable surface is required to maintain a stable EDL structure. Considering these factors, a highly doped n-Si(100) single-crystal wafer with a native oxide layer was chosen as the working electrode. Figure 2a shows the NR profile of Si electrode measured in air. As the average and maximum values of relative error of reflection intensity were 3% and 9%, respectively, error bars are omitted in the NR profile. The NR profiles seem to decrease monotonously according to q^{-4} , indicating that both the Si/native oxide layer interface and the oxide layer surface are atomically smooth, and the native oxide layer is very thin. A fitting analysis was carried out using MOTOFIT³⁴ (The fitting result is shown in Fig. S1 (available online at stacks.iop.org/ECSA/1/020503/mmedia)). The structural parameters for Si and native oxide are as follows. The roughness of the Si surface was 4.41 Å. The thickness and roughness of native oxide are 10.93 Å and 3.66 Å, respectively. The thickness was within values reported previously.^{35,36} These values were used in the analysis of EDL structure.

Figure 3 shows a typical cyclic voltammogram (CV) of n-Si(100) electrode measured in *d*-[BMIM]TFSA using the NR-cell. The electrode was scanned between -1.2 and $+0.4$ V. Outside of this potential range, the observed current rapidly increased; therefore, we defined this potential range as an electrochemical window. In this electrochemical window, even the current value is small, a small anodic and cathodic current were observed. Most of the observed current was owing to the (dis)charge of EDL. The observed current at $E < -1.0$ V and $E > 0.3$ V may be owing to the residual water in the *d*-[BMIM]TFSA and the electrochemical oxidation of *d*-[BMIM]TFSA, respectively. In this study, we attempted to analyze the EDL structure at $E = -1.2$ V, which is the negative limit of the electrochemical window. The EDL structure at negative potential is important for electrodeposition reactions since electrodeposition was carried out under diffusion limit conditions, i.e., at the potential, which is far from the redox potential.

Figure 2b shows the NR profile measured at $E = -1.2$ V, which is the negative limit of the electrochemical window. As the average and maximum values of relative error of reflection intensity were 4% and 11%, respectively, error bars are also omitted in the NR profile. Due to the incoherent scattering by the hydrogen atoms in the ionic

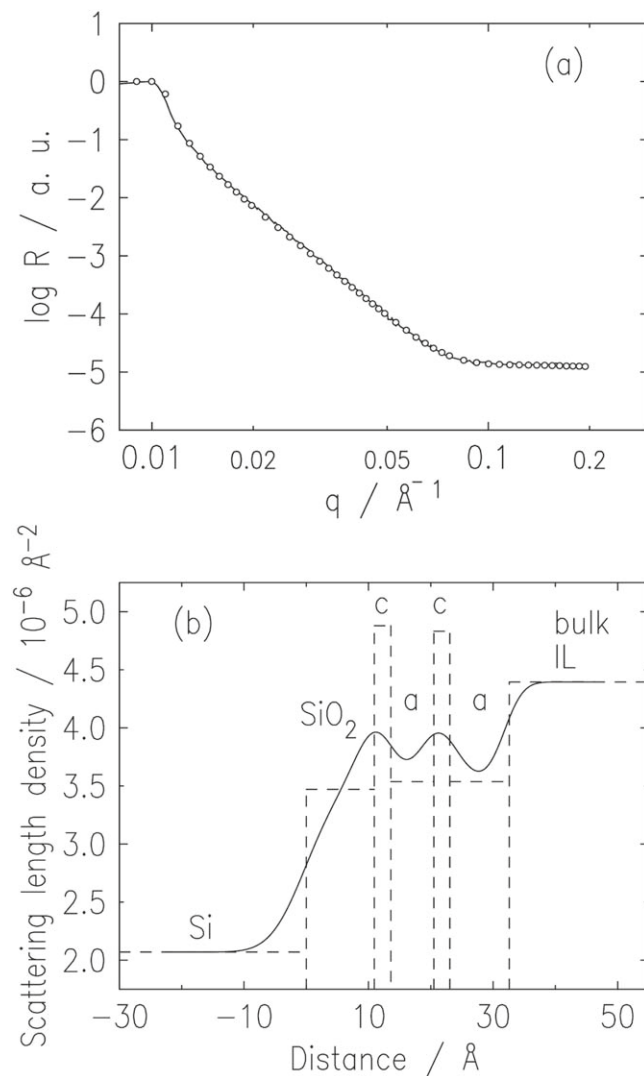


Figure 5. (a) Reflectivity profile measured at $E = -1.2$ V (circle) and the fitted result (solid line) and (b) SLD profile elucidated by parameter fitting: cation and anion were denoted by c and a, respectively.

liquid, this sample system suffers from a strong featureless background (1.3×10^{-5}). At $E = -1.2$ V, a cathodic current was observed in the CV shown in Fig. 3, however, the stationary current during the NR measurement was smaller than 60 nA cm^{-2} . In the NR profile, an obvious oscillation was not observed; however, the difference was clearly observed between NR profile measured at $E = -1.2$ V and simulated for a bulk structure model, suggesting that there is a specific structure of IL molecules adsorbed onto the electrode surface. If the IL molecules do not form any specific structure, the reflectivity monotonously decreases with q^{-4} .

To elucidate the exact structure that [BMIM]TFSA molecules form in EDL, parameter fittings were carried out using MOTOFIT. In the fitting procedures, the anion-cation pair layered model was adopted. Concerning the number of layers in the fitting procedure, we previously deduced the number of layers with fully deuterated [BMIM]TFSA and reported that two anion-cation pairs were stacked on a Si(100) electrode.²⁴ Further, Begic et al. previously reported the dependence of the EDL structure on the surface charge using MD simulation.³⁷ In their study, the EDL structure of 1-butyl-3-methylimidazolium dicyanamide ([BMIM]dca) was simulated and was reported that at the surface charge of $0.02 e \text{ atom}^{-1}$ two anion-cation pairs are stacked. The viscosity of [BMIM]dca and [BMIM]TFSA is 27.34 and 51.1 mPa·s at 25 °C.^{38,39} The melting point of [BMIM]dca and [BMIM]TFSA is -6 and -2 °C.⁴⁰ Both the viscosity and the

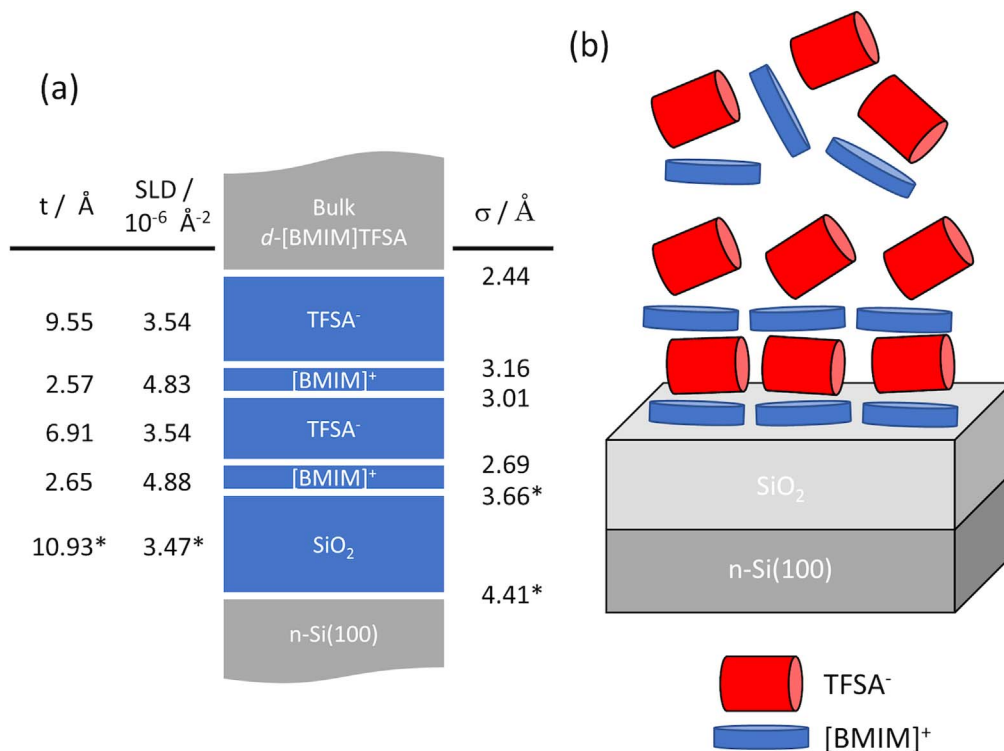


Figure 6. (a) EDL structure obtained by parameter fitting; t is thickness. σ is roughness. Fixed parameters are shown as * and (b) its schematic representation.

melting point reflect the anion-cation interaction and both the dca^- and $TFSA^-$ have a molecular structure in common, suggesting that the interaction of dca^- and $TFSA^-$ with $[BMIM]^+$ is roughly equal. Therefore, their simulation can be of reference to our results. We evaluated the surface charge of $[BMIM]TFSA/n-Si(100)$ interface at $E = -1.2$ V. We carried out EIS measurements with non-deuterated $[BMIM]TFSA$ to elucidate the flat-band potential (E_{fb}) and the capacitance of the space charge layer formed in Si electrode (Fig. S3) and the capacitance of the native oxide layer at $E = -1.2$ V. We deduced the E_{fb} using a Mott-Schottky plot of the capacitance of the space charge layer; however, an E_{fb} was not obtained owing to the uniquely large hysteresis, originating from the imperfect structure of the native oxide layer.⁴³ At this point, it was determined that the E_{fb} is between $E = -0.43$ and 0.19 V. The capacitance of the native oxide layer was approximately $2 \mu F cm^{-2}$. The potential applied to the Si(100) surface was $E - E_{fb}$. As previously described, the E_{fb} could not be exactly obtained, therefore, the surface charge can be finally estimated to be $2.27 \pm 0.31 \mu C cm^{-2}$, which corresponding to $0.021 \pm 0.003 e atom^{-1}$. As described above, the study by Begic et al. reported that at the surface charge of $0.02 e atom^{-1}$ two anion-cation pairs are stacked.³⁷ This model is the same as we experimentally elucidated in our previous study. Therefore, In our parameter fitting, we mainly focused on the two-anion-cation pair model and to check the validity of the structure model, all the zero, one, and three-anion-cation pair models were also carefully tested.

In each model, both cases, in which the first layer was either $d-[BMIM]$ or $TFSA^-$, were tested. As for the inner structure of the $d-[BMIM]$ cation layer, three orientations were tested, imidazole ring down, butyl group down, and edge-on (Figs. S4 and S5). As described in the introduction, if there is enough contrast of SLD values inside a molecule, it is possible to distinguish the orientation

of the molecules. Figure 4 shows the simulation of NR profiles with $d-[BMIM]TFSA$ synthesized in this study. Cases of imidazole ring down, butyl group down, and edge-on structures were simulated. In this simulation, the number of anion-cation pairs was two and the roughness of each $[BMIM]TFSA$ molecule layer was 3.66 \AA , which corresponds to the roughness of the native oxide surface. In the imidazole ring down and butyl group down structures, $TFSA^-$ anions are perpendicularly orientated to the surface. In the edge-on structure, $TFSA^-$ anions are horizontally oriented to the surface. Figure 4 shows that three NR profiles have different features, e.g., the position of the peak and the amplitude of oscillation, indicating that the orientation of $[BMIM]TFSA$ molecules in the EDL can be explicitly distinguished by NR profiles.

The parameter fitting results are shown in Fig. 5a as a solid line and the SLD profile is shown in Fig. 5b. In parameter fittings, the structural parameters of the Si surface and native oxide film were fixed, and they are elucidated using NR as described above. The thickness, SLD value, and roughness of each layer were fitted. The structure model, which gave the minimum χ^2 and was physically consistent, was a two anion-cation pair model starting with a $d-[BMIM]$ layer. The orientation of a $d-[BMIM]$ molecule was edge-on. The detailed parameters are shown in Fig. 6. In Fig. 5b, the SLD value is smaller than bulk IL owing to the overlapping of the native oxide, $d-[BMIM]$, and $TFSA^-$ layers (see Fig. S6).

To further discuss the inner structure of both $[BMIM]$ and the $TFSA^-$ layer, we calculated the stable forms of the $[BMIM]$ cation and the $TFSA^-$ anion using MOPAC (AM1 or PM3 Hamiltonian and EF method were used). The most stable form of the $[BMIM]$ cation occurs when both the imidazole ring and the butyl group lie in the same plane with a thickness of approximately 2.4 \AA (Fig. S7a). The diameter of the imidazole ring is approximately 4.1 \AA . Therefore, the fitting result suggests that in the first $[BMIM]$ cation layer, which is directly formed on the electrode surface, the imidazole ring parallels to the electrode surface and the butyl group lies in the same plane. Previous studies using the sum-frequency generation technique^{44,45} and MD calculation show a similar tendency,⁴⁶ though both the anion of IL and the electrode material are different in these studies. Taking this orientation may maximize the interaction between the

delocalized electron in the imidazolium ring and the surface charge. The orientation of [BMIM] cation molecules in the second layer is the same as the first layer and allows the packing of counter-ions at higher densities.³⁷

As for TFSA anion, it was reported that the most stable conformation is a *transoid* form,⁴⁷ in which the charge is mainly localized on the O and N. The appearance of TFSA anion is approximated to be the cylindrical form with an approximate diameter of 6.6 Å and an approximate length of 10.4 Å (Fig. S7b). The thickness of the first anion layer was 6.91 Å and agrees with the diameter of the TFSA anion, indicating that in the first TFSA anion layer, TFSA anions are also horizontally oriented to the surface. In the *transoid* form, the CF₃ group does not sterically hinder the Coulomb interaction between the SO₂ group and the imidazolium ring. Whereas the thickness of the second anion layer was 9.55 Å. This thickness indicates that the orientation of TFSA anion is about 20° to the surface according to a geometric calculation. It suggests that the second TFSA anion layer has the structure between the layered structure and the bulk structure since the screening length is short owing to the small surface charge.

Summary

In summary, the structure of the [BMIM]TFSA/Si(100) electrode interface at a negative potential was studied using NR. To elucidate the EDL structure with the orientation of adsorbed molecules precisely, we synthesized partially deuterated [BMIM]TFSA. In the [BMIM]⁺ molecule, the butyl group had a close SLD value to a TFSA anion. Our NR measurements uncovered that the [BMIM] TFSA molecules form a layered structure on the n-Si(100) surface and the molecules in the first three layers are horizontally oriented to increase the interaction between the cation and anion molecules. Our results show that not only the structure of the layer adsorbed on the surface but also that far from the surface can be analyzed using the NR technique. Further, they also indicate that the NR technique using ILs with precisely controlled deuteration is an effective analysis method for the structural study of the EDL formed at the IL/electrode interface.

Acknowledgments

This work was supported by JSPS KAKENHI Grant Number 15K05402. The neutron experiment at the Materials and Life Science Experimental Facility of the J-PARC were performed under a user program (Proposal No. 2016A0040 and 2017B0010). The National Deuteration Facility is partly funded by the National Collaborative Research Infrastructure Strategy (NCRIS), an initiative of the Australian government. Deuterated samples were prepared at the National Deuteration Facility at the Australian Nuclear Science and Technology Organization (Proposal No. NDF6142). The sample preparation of neutron experiments was conducted at the User Experiment Preparation Lab III (CROSS) and the deuteration laboratory (J-PARC MLF).

ORCID

Kazuhisa Tamura  <https://orcid.org/0000-0002-8338-485X>

References

1. H. Ohno, *Electrochemical Aspects of Ionic Liquids* (Wiley, Hoboken, NJ) (2005).
2. M. Watanabe, M. L. Thomas, S. Zhang, K. Ueno, T. Yasuda, and K. Dokko, *Chem. Rev.*, **117**, 7190 (2017).
3. C. F. J. Francis, I. L. Kyratzis, and A. S. Best, *Adv. Mater.*, 1904205 (2020).

4. M. B. Karimi, F. Mohammadi, and K. Hooshyari, *Phys. Chem. Chem. Phys.*, **22**, 2917 (2020).
5. M. Shimizu, K. Yamaguchi, H. Usui, N. Ieuji, T. Yamashita, T. Komura, Y. Domi, T. Nokami, T. Itoh, and H. Sakaguchi, *J. Electrochem. Soc.*, **167**, 070516 (2020).
6. L.-G. Lin, J.-W. Yan, Y. Wang, Y.-C. Fu, and B.-W. Mao, *J. Exp. Nanosci.*, **1**, 269 (2006).
7. Z. Liu, N. Borisenko, S. Zein El Abedin, and F. Endres, *J. Solid State Electrochem.*, **18**, 2581 (2014).
8. Y.-C. Fu, Y.-Z. Su, H.-M. Zhang, J.-W. Yan, Z.-X. Xie, and B.-W. Mao, *Electrochim. Acta*, **55**, 8105 (2010).
9. Y.-C. Fu, J.-W. Yan, Y. Wang, J.-H. Tian, H.-M. Zhang, Z.-X. Xie, and B.-W. Mao, *J. Phys. Chem. C*, **111**, 10467 (2007).
10. Y. Zheng, *Int. J. Electrochem. Sci.*, **11**, 9585 (2016).
11. M. V. Fedorov and A. A. Kornyshev, *Chem. Rev.*, **114**, 2978 (2014).
12. M. Mezger et al., *Science*, **322**, 424 (2008).
13. Y. Lauw, M. D. Horne, T. Rodopoulos, V. Lockett, B. Akgun, W. A. Hamilton, and A. R. Nelson, *Langmuir*, **28**, 7374 (2012).
14. N. Nishi, J. Uchiyashiki, Y. Ikeda, S. Katakura, T. Oda, M. Hino, and N. L. Yamada, *J. Phys. Chem. C*, **123**, 9223 (2019).
15. M. Chu, M. Miller, T. Douglas, and P. Dutta, *J. Phys. Chem. C*, **121**, 3841 (2017).
16. R. Atkin, N. Borisenko, M. Drüschler, F. Endres, R. Hayes, B. Huber, and B. Roling, *J. Mol. Liq.*, **192**, 44 (2014).
17. N. Nishi, Y. Hirano, T. Motokawa, and T. Kakiuchi, *Phys. Chem. Chem. Phys.*, **15**, 11615 (2013).
18. K. Motobayashi, Y. Shibamura, and K. Ikeda, *Electrochem. Commun.*, **100**, 117 (2019).
19. W. Zhou, S. Inoue, T. Iwahashi, K. Kanai, K. Seki, T. Miyamae, D. Kim, Y. Katayama, and Y. Ouchi, *Electrochem. Commun.*, **12**, 672 (2010).
20. A. A. Kornyshev, *J. Phys. Chem. B*, **111**, 5545 (2007).
21. M. Giroto, T. Colla, A. P. Dos Santos, and Y. Levin, *J. Phys. Chem. B*, **121**, 6408 (2017).
22. K. Tamura, S. I. Miyaguchi, K. Sakaue, Y. Nishihata, and J. Mizuki, *Electrochem. Commun.*, **13**, 411 (2011).
23. K. Tamura and Y. Nishihata, *The Journal of Physical Chemistry C*, **120**, 15691 (2016).
24. K. Akutsu-Suyama, M. Cagnes, K. Tamura, T. Kanaya, and T. A. Darwish, *Phys. Chem. Chem. Phys.*, **21**, 17512 (2019).
25. J. Als-Nielsen and D. McMorrow, *Elements of Modern X-ray Physics* (Wiley, New York) (2001).
26. H. Kawaura, M. Harada, Y. Kondo, H. Kondo, Y. Suganuma, N. Takahashi, J. Sugiyama, Y. Seno, and N. L. Yamada, *ACS Appl. Mater. Interfaces*, **8**, 9540 (2016).
27. M. Hirayama, M. Yonemura, K. Suzuki, N. Torikai, H. Smith, E. Watkinsand, J. Majewski, and R. Kanno, *Electrochemistry*, **78**, 413 (2010).
28. M. Ooe, K. Miyata, J. Yoshioka, K. Fukao, F. Nemoto, and N. L. Yamada, *J. Chem. Phys.*, **151**, 244905 (2019).
29. K. Miyamoto, N. Hosaka, M. Kobayashi, H. Otsuka, N. Yamada, N. Torikai, and A. Takahara, *Polym. J.*, **39**, 1247 (2007).
30. P. A. Fiorito, W. A. Alves, F. F. C. Bazito, F. E. Haber, G. Froyer, S. I. C. de Torresi, and R. M. Torresi, *Electrochim. Acta*, **53**, 7396 (2008).
31. M. Yonemura, M. Hirayama, K. Suzuki, R. Kanno, N. Torikai, and N. L. Yamada, *J. Phys. Conf. Ser.*, **502**, 012054 (2014).
32. M. N. Kobrak, *Green Chem.*, **10**, 80 (2008).
33. V. F. Sears, *Neutron News*, **3**, 26 (2006).
34. A. Nelson, *J. Appl. Crystallogr.*, **39**, 273 (2006).
35. M. Morita, T. Ohmi, E. Hasegawa, M. Kawakami, and M. Ohwada, *J. Appl. Phys.*, **68**, 1272 (1990).
36. Y. Yang, "Synchrotron X-ray diffraction studies on oxide surfaces and interfaces." *PHD Thesis*, The University of Michigan (2014).
37. S. Begic, E. Jonsson, F. Chen, and M. Forsyth, *Phys. Chem. Chem. Phys.*, **19**, 30010 (2017).
38. K. R. Harris, M. Kanakubo, and L. A. Woolf, *J. Chem. Eng. Data*, **52**, 1080 (2007).
39. M. Larriba, P. Navarro, J. Garcia, and F. Rodriguez, *Ind. Eng. Chem. Res.*, **52**, 2714 (2013).
40. C. P. Fredlake, J. M. Crosthwaite, D. G. Hert, S. N. V. K. Aki, and J. F. Brennecke, *J. Chem. Eng. Data*, **49**, 954 (2004).
41. M. Chemla, V. Bertagna, R. Erre, F. Rouelle, S. Petitdidier, and D. Levy, *Appl. Surf. Sci.*, **227**, 193 (2004).
42. M.-G. Li, L. Chen, Y.-X. Zhong, Z.-B. Chen, J.-W. Yan, and B.-W. Mao, *Electrochim. Acta*, **197**, 282 (2016).
43. P. Schmuki, H. Bohni, and J. A. Bardwell, *J. Electrochem. Soc.*, **142**, 1705 (1995).
44. C. Aliaga and S. Baldelli, *J. Phys. Chem. B*, **110**, 18481 (2006).
45. S. Rivera-Rubero and S. Baldelli, *J. Phys. Chem. B*, **108**, 15133 (2004).
46. E. Paek, A. J. Pak, and G. S. Hwang, *J. Electrochem. Soc.*, **160**, A1 (2012).
47. K. Fujii, T. Fujimori, T. Takamuku, R. Kanzaki, Y. Umebayashi, and S. Ishiguro, *J. Phys. Chem. B*, **110**, 8179 (2006).